# 13. MEASURES FOR RADIATION PROTECTION

## 13.1 Beam Loss in Superconducting Magnets

A basic problem of superconducting accelerators and storage rings is the extent to which the magnet system must be shielded from beam losses. Relatively small fractions of the total beam can cause superconducting magnets to quench. The recovery time required is not negligible.

Conventional accelerators and storage rings do lose beam, as attested to by the residual radioactivity of their magnet systems and by experimental observation of both slow and catastrophic intensity reductions through failure of equipment, beam blowup or in the course of tune-up procedures. Certain processes, such as resonant extraction and beam scraping to clean up phase space are inherently lossy and can be described reasonably accurately. Other processes, such as single-turn injection, single-turn extraction, acceleration and storage, are in principle "loss-free." Experience has proved these processes do not work perfectly, and one must try to minimize such accidental beam-loss effects on the superconducting magnet system.

## 13.2 Tolerable Level of Energy Deposition

Primary beam protons or their secondary shower products that hit and interact with the superconducting coils will cause local energy deposition in the conductor through ionization loss. This energy, if not removed, will heat the superconductor to the normal transition temperature and thus cause the magnet to quench. The temperature allowed above the nominal operating point of 4.6 K is related to the product of magnetic field and current in the conductor. At high excitation, near quench limit, only fractions of a degree K

temperature difference can be tolerated, whereas at the zero-current field limit, the conductor must be elevated to approximately 10 K in order to reach the normal domain. The critical field $B_c$ and current density $J_c$ are related to the temperature by $(J_c \cdot B_c)^{\frac{1}{2}} \propto (10^\circ - T)$. For a particular magnet that at 4.6 K has a maximum current and field operating point of $I_{max} B_{max}$, the allowable temperature difference is then related to the operating point by

$$\Delta T(^\circ K) \simeq (10^\circ - 4.6^\circ)\left[1 - \left(\frac{I \cdot B}{I_{max} \cdot B_{max}}\right)^{\frac{1}{2}}\right].$$

The temperature change resulting from energy deposition is related to the time dependence of the loss. At one extreme, an instantaneous loss $\Delta E$ will result in a temperature change given by the integral of the specific heat of the conductor

$$\Delta E = \int_{4.6^\circ}^{T_{final}} C_p(T)dT.$$

At the other extreme, for a slow (> 100 ms) uniform loss, the conductor-helium system will be in equilibrium, with heat transfer taking place from the conductor through the cable insulation to the helium, which is assumed in this limiting case to be boiling. For loss times of the order of a millisecond, an intermediate condition exists where very high heat transfers to the helium inside the insulation might exist for a short time. The amount of energy deposition that can be tolerated according to models[1] for these different time domains is shown in Fig. 13-1, together with experimental results of measurements on magnets,[2,3] interpreted with the help of shower calculations. As expected, at peak excitation the allowable energy deposition

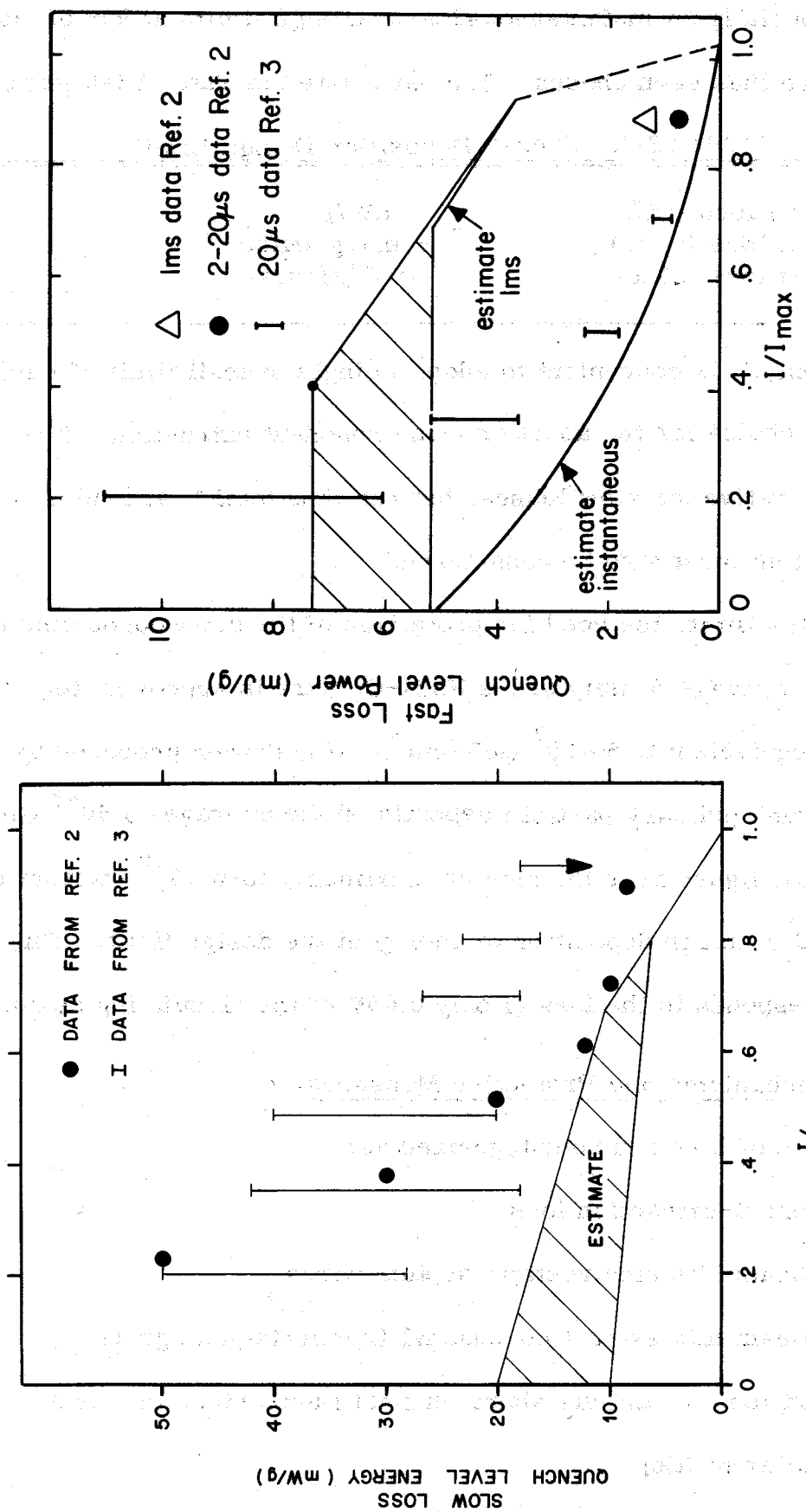


Fig. 13-1. Tolerable energy deposition in superconducting coils.

is small, especially for instantaneous loss. Design limits at 90% of maximum excitation have thus been chosen. They are listed in Table 13-I below.

Table 13-I. Energy Deposition Design Limits

| | |
|---|---|
| slow loss (DC) | 8 mW/g |
| fast loss (1 ms) | 1 mJ/g/pulse |
| fast loss (20 $\mu$s) | $\frac{1}{2}$ mJ/g/pulse |

For the present, it is convenient to adopt a single overall limit of 1 mJ/g. It is a proper choice for the abort or 1-ms resonant extraction. It is slightly conservative for slow losses, but here the total heat load in the cryogenic system must also be considered.

With this limit, the need for protection of the superconducting magnets is clear. The average density of the NbTi-Cu wire is approximately 8 g/cm$^3$, so 1 mJ/g is equivalent to $5 \times 10^7$ GeV/cm$^3$. If a shower produced by a single interacting primary particle deposits on the average $5 \times 10^{-3}$ GeV/cm$^3$, to take a typical figure near the shower maximum, then $10^{10}$ interacting primaries will result in deposition of energy at the design limit. This situation corresponds to the loss of only 0.05% of the circulating beam.

## 13.3 Loss Mechanisms and Protective Measures

The kinds of loss can be categorized as:

(i) Resonant-extraction loss

  a) Beam hits electrostatic septum wires

  b) Beam hits extraction-channel Lambertson magnets

(ii) Abort loss; beam hits abort-channel Lambertson magnets [similar to (i)b]

(iii) Injection first-turns loss; beam is mis-steered into magnets

(iv) Betatron-space blow-up; beam hits scraper system

(v) Off-momentum loss; beam hits momentum scraper system

The possible protective measures can be categorized as:

(i) Scraper system

a) Beam scraper and collimator system in long straight sections with conventional bending magnets and momentum analysis

b) Beam scraper systems in medium straight sections for off-momentum loss

c) Plugs in specific superconducting magnets downstream of bad loss points

d) Beam scrapers in superconducting magnets throughout the accelerator

(ii) Electronic - alarms and abort

a) Position detectors, alarms

b) Loss monitors, alarms

c) Tune and coherent-oscillation detectors

d) Device-failure alarms

e) Abort

## 13.4 The Extraction-Loss Problem

In the resonant-extraction process, individual-particle amplitudes grow at a rate that increases with amplitude. For efficient extraction the final step size, when particles pass through the field region of the

electrostatic septum, is of the order of the septum wire-to-cathode gap and the probability that any particle hits the septum wires is approximately $2W/\Delta$, where W is the wire thickness (approx. 2 mils) and $\Delta$ is the two-turn step size or wire-cathode spacing (approx. 400 mils). It is expected that 1 to 2% of the beam will hit septum wires during extraction. These wires are 2-mil tungsten spaced every 0.1 in. along the length of the septum (two modules, each 12 ft long). Particles that hit the septum wires at D0 can be considered as a uniform parallel beam perfectly aligned with the septum wires. As they proceed along the septum, they can either undergo nuclear interactions, multiply scatter out, or pass through all wires. Typical angles for multiple Coulomb scattering and coherent nuclear elastic scattering are 40 $\mu$rad and these particles will propagate around to the extraction channel at A0, where they will either be (a) extracted, (b) hit the Lambertson septum, (c) continue around the accelerator and be extracted two turns later or (d) be lost in the accelerator. Those lost in the accelerator or in the Lambertson will shower and produce radiation in the downstream superconducting magnets.

Protons that undergo nuclear interactions in the electrostatic septum will similarly produce radiation in the magnets downstream of the straight section. For the present purposes this radiation can be characterized by three components:

(1) high-energy protons with energies above 500 GeV

(2) neutral secondaries from $\pi^0$ decay

(3) low-energy (< 500 GeV) charged secondaries.

If shielding is not placed between the septum and the superconducting magnets, the three components have the following effects:

(1) High-energy protons will continue quite a way in the aperture of the superconducting magnets before being bent into the inside wall. They carry substantial energy and produce substantial energy deposition over considerable distance.

(2) Neutrals proceed straight ahead as the magnets bend away from them horizontally and, because they are reasonably well collimated, tend to produce a peak in the energy density roughly where they intersect the vacuum wall.

(3) Charged secondaries are bent into the magnets quickly in the first few meters.

(4) There is a sharp peak at the front of the magnet string from any particles with large enough angle to hit the magnet's front face.

Figure 13-2 illustrates these components.

Significant reduction in energy deposition can be made by incorporating an orbit-bump magnetic analyzer and collimator scheme with the electrostatic septum in the D0 straight section. Figure 13-3 illustrates this scheme. Four conventional (perhaps Main-Ring) bending magnets are arranged to produce a vertical orbit kink. Inside these magnets are placed collimators of dimensions determined by the injected beam emittance, the resonant-extracted horizontal beam size, and the relative betatron-amplitude functions at the various magnet locations. Care is taken to ensure that under normal operation the upstream collimators are the aperture stops and that

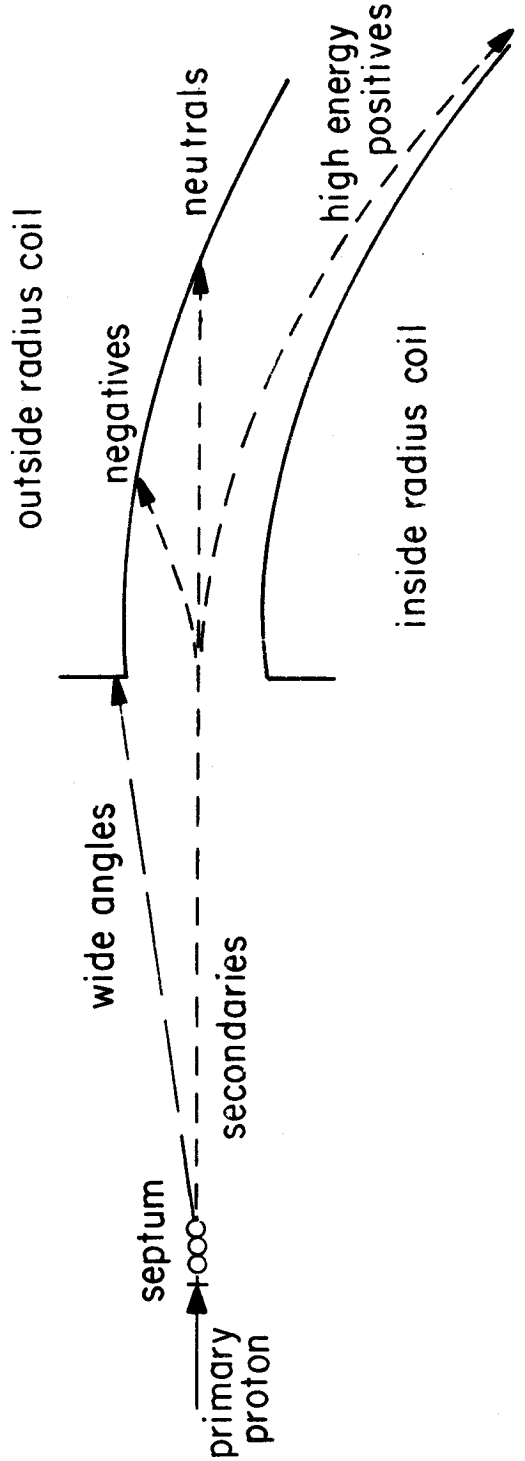


Fig. 13-2. Radiation components from nuclear interactions.

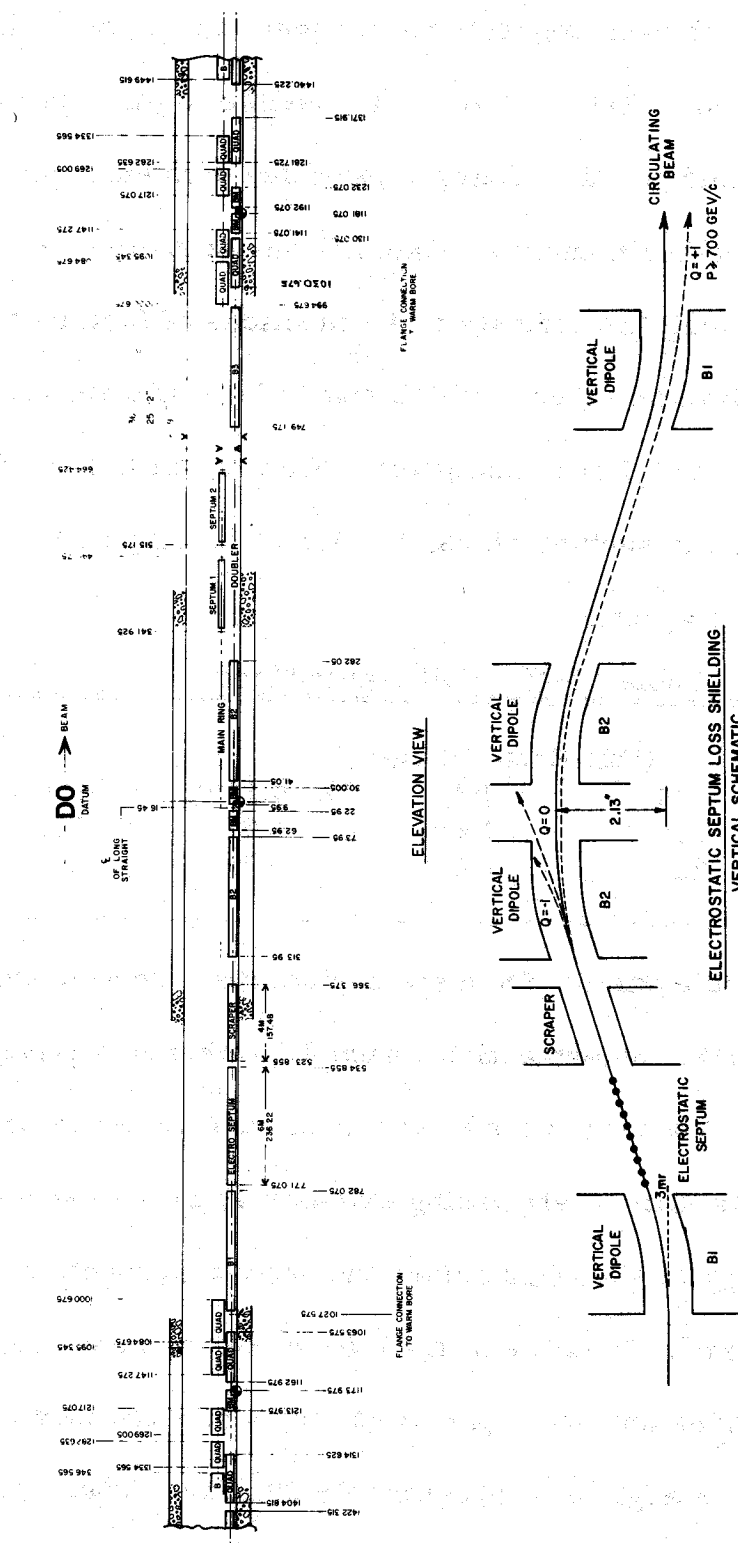


Fig. 13-3. Layout of D0 long straight section.

primary beam never scrapes on the downstream collimators or superconducting-magnet beam plugs. With each conventional magnet bending by 3 mrad and with collimator sizes as given in Table 13-II, it is possible to intercept all neutral and negative particles and positive-charged particles with energies below approximately 75% of the beam energy. Calculations of shower energy density in the superconducting magnets indicate that reductions of factors of 20 to 50 are gained by this collimator scheme which should be sufficient for 1-ms resonant extraction of 2 to 5 $\times 10^{13}$ per pulse. That is, with 2% of 2 to 5 $\times 10^{13}$ protons hitting the septum wires, 1 mJ/g of heating will be produced in the superconducting magnets.

Table 13-II. Collimator Sizes

| | (Full Width in cm) | | | | |
|---|---|---|---|---|---|
| | B1 | B2 | B3 | Quad Plug | Bend Plug |
| Horiz. | 7.5 | 5.0 | 3.4 | 4.0 | 5.0 |
| Vertical | 1.6 | 2.2 | 4.0 | 6.0 | 4.0 |

Multiply scattered particles from the septum that proceed around half the accelerator and strike the extraction-channel Lambertson septa behave in two different ways. Those that strike the front surface of the first magnet septum have good probability of showering extensively in the septum steel and considerable energy is absorbed before the shower products reach the superconducting elements. Because of the lattice optics, however, the beam is horizontally converging and some particles may graze the long side of the magnetic septum with an angle of approximately 30 $\mu$rad. These produce 10 times more radiation in the downstream superconducting string. The radiation protection measures planned in A0 are:

(i) a 2-m collimator at the downstream end of the straight section.

(ii) the Lambertson magnet septa, built wider at the upstream end to reduce the number of particles that can hit with grazing incidence.

It should be possible for $10^{11}$ particles to hit the Lambertson without exceeding the 1 mJ/g limit in downstream magnets. A plug or thick-walled vacuum chamber placed within the downstream superconducting magnets will further raise this limit.

## 13.5 The Abort Problem

The abort extraction channel incorporates a magnetic analyzer-collimator system similar to that at D0. Detailed calculations of this geometry have not been done, but we expect that a few times $10^{11}$ to $10^{12}$ protons can be lost at C0 in the abort process without quenching the nearby magnets. Here the particles hitting the septum are those that have grown to a large phase space before the kicker is fired and thus hit the septum at the abort time.

Beam scrapers at the upstream ends of C0 and D0 straight sections will be used in conjunction with the orbit kinks in these straight sections to act as limiting aperture restrictions for large betatron oscillations and for halo scrapers during colliding-beam experiments.

## 13.6 Calculations of Energy Deposition in Magnets

A study is in progress to calculate the distribution of energy deposition in the superconducting magnets for the various complicated geometries of the accelerator system. The program CASIM[4] has been modified to include the geometry of the magnet configurations and the presence of the electric and magnetic fields of septa and magnets.

The calculations are not complete, but a number of configurations have been analyzed.[5] They have been made only for 1000-GeV protons and the only material considered so far for scrapers, collimators, and plugs has been iron. We give some examples for illustrative purposes of energy deposited in the median plane of the superconducting magnets. Figure 13-4 shows the bin subdivision of the coils used in the calculations. Here we only display data from the cross-hatched region. Inward and outward regions in the ring are specified at "inside radius" and "outside radius", as shown in Figure 13-2.

In Fig. 13-5, results are given for a simplified geometry of the D0 straight section that does not include superconducting quadrupoles at the upstream end of the superconducting bend string. The curves show energy deposition in the median-plane coil regions of the superconducting bends as a function of distance along the bends per proton incident on the electrostatic-septum wires. The different conditions of the curves are:

(i) No shielding; no conventional bend magnets.

(ii) Septum upstream of four bend magnets. The first magnet bends horizontally inward. Collimators in the magnets are $5.6 \times 2$ cm$^2$. (h x v)

(iii) Septum is downstream of the first bend magnet, which bends inward. The momentum difference $\Delta p$ from the primary momentum, which gets through the conventional system, should be about half that of (ii).

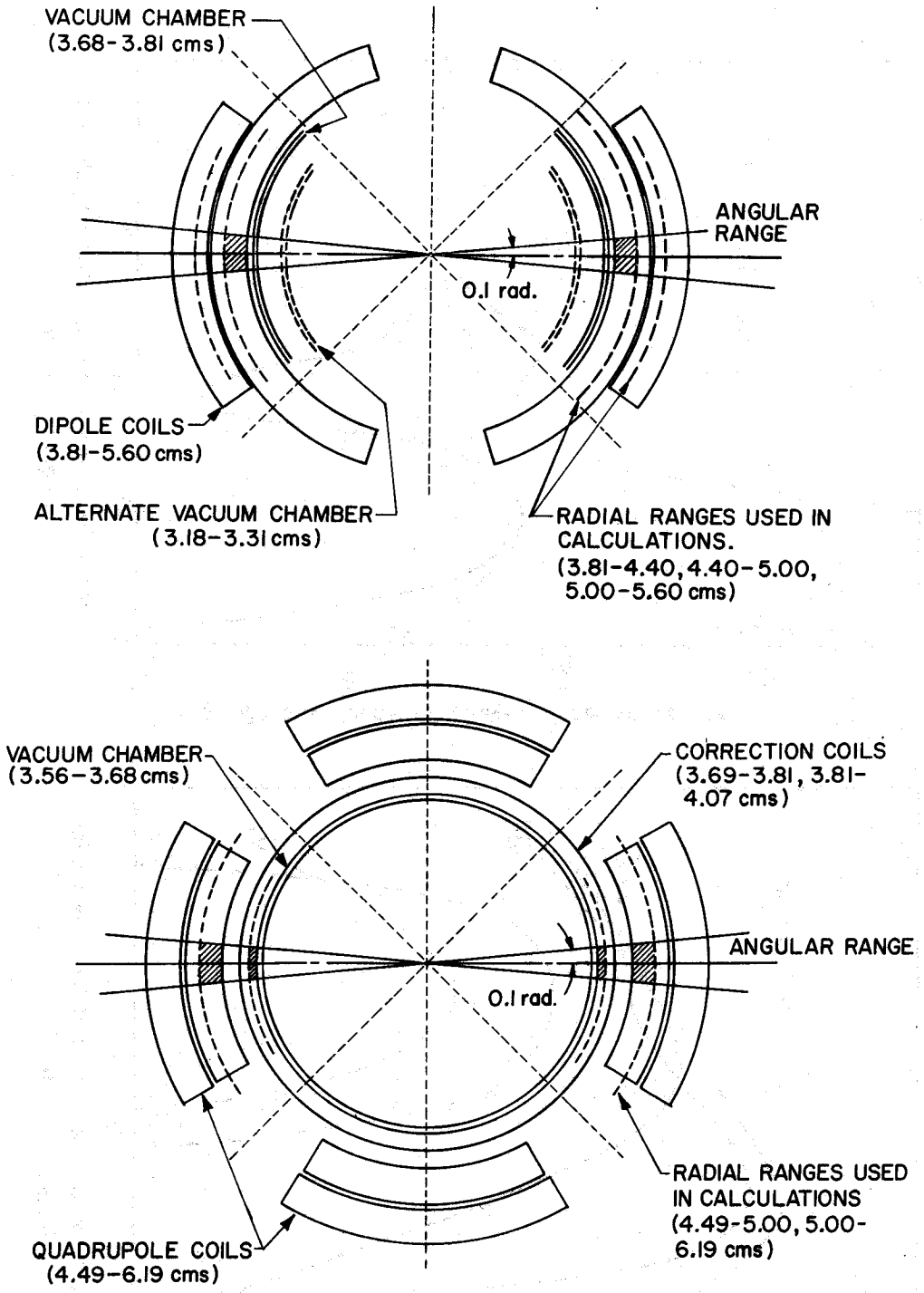


Fig. 13-4. Dipole and quadrupole coil geometry used for energy deposition calculations. Crosshatching indicates regions discussed here.

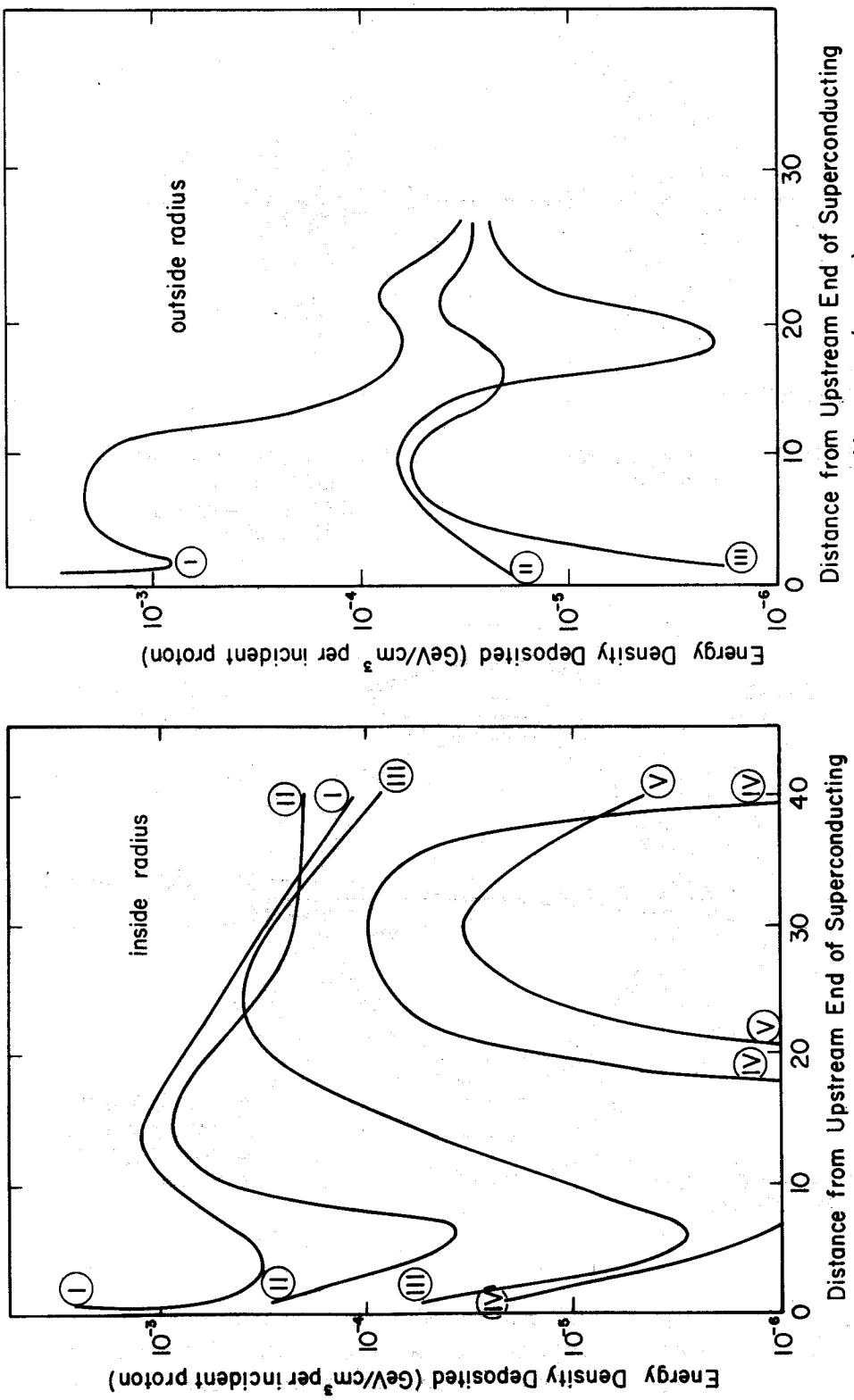


Fig. 13-5. Energy deposition downstream of the D0 septum.

(iv) The septum is downstream of the first bend, which now bends vertically. The momentum difference cutoff is further reduced because the vertical aperture of the collimator is smaller than its horizontal aperture.

(v) A plug (5 ×3 cm) has been put in the superconducting magnets. It extends to the coil surface. A further small reduction in in energy density is achieved.

It appears that a reduction of a factor 50 has been obtained and curves of energy density on the inside-radius coil surface clearly show effects of increasingly better momentum selection. The energy deposition on the outside-radius coil surface is greatly reduced by a beam bump and does not present a problem. In the case of the vertical bump, care must be taken in the way the results are interpreted because we no longer have up-down symmetry. The inside-radius coil at the midplane may not be the location of the energy-density maximum; this location is expected to vary with distance along the magnets. Further investigation indicates that the maximum energy density may exceed that at the inside median plane by as much as a factor of two.

We have also investigated a more realistic geometry including the superconducting quadrupoles and collimators of size given in Table 13-II. Results are very similar to the above. Further calculations are required to optimize the plug geometry.

Figure 13-6 illustrates the energy deposition in a medium straight section from a scraper downstream of the quadrupole for cases with no

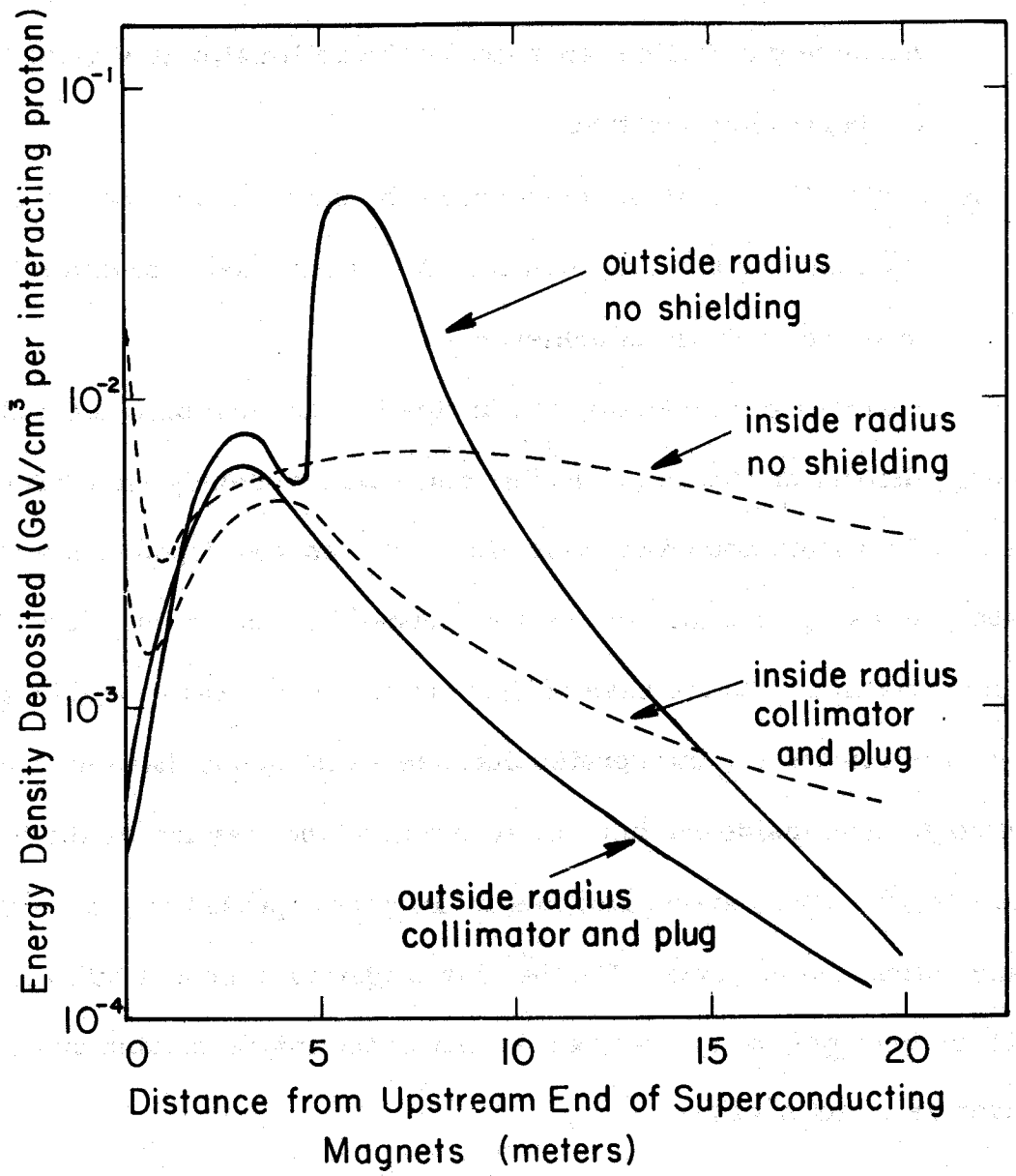


Fig. 13-6. Energy deposition in magnets downstream of a scraper in a medium straight section.

shielding and with a 2-m collimator upstream and a plug in the superconducting magnets, both with 5 ×3 cm aperture. The absorption of the neutral peak by the plug is clearly illustrated; the reduction of energy from charged particles is smaller, but can still be seen.

We have also considered the case of beam striking a Lambertson magnet in a long straight section. With a parallel incident beam uniformly distributed over the septum region for a height of ± 1 mm, we find peak energy densities of $4 \times 10^{-4}$ GeV/cm$^3$ per incident particle in the downstream superconducting bending magnet. If the incident particle strikes the side with a glancing angle of 30 μrad, energy densities of $3 \times 10^{-3}$ GeV/cm$^3$ result. There is no magnet plug included in these calculations.

Other cases are being considered in this work, but have not yet been completed.

## 13.7 Status of Shielding Design

Simulation of the process of a particle circulating in a synchrotron until it hits the edge of a scraper and produces a shower is a complicated problem involving both particle dynamics in an accelerator and the multiple-scattering, nuclear-interaction and shower-development processes of a particle near the edge of an absorber.

An attempt to model the behavior described above is in progress in order to determine the amount of energy characteristically absorbed in the scraper, as opposed to that deposited in downstream superconducting magnets. A conservative design that does not rely on this analysis assumes that the scraper acts only as a source in which nuclear interactions occur

and does not in itself absorb or develop the shower. It is clear under these guidelines that scraper systems are best implemented in long straight sections C0 and D0, where the conventional bumps can provide shields, as discussed above. Using the electrostatic-septum calculations as a guide, we would guess that at least $2 \times 10^{11}$ particles could interact in a scraper without exceeding 1 mJ/g energy deposition in the superconducting magnets.

Off-momentum protons may not hit the scrapers in the long straight sections because the dispersion function $\eta$ is one-third its maximum value at these locations. At medium straight sections, (Locations 17) $\eta$ is a maximum and scrapers can be installed. There is not, however, sufficient space for magnetic shields as used in C0 and D0, so that the scraper acts mainly as a source for interactions and the downstream drift space allows the secondary beam to diffuse. Calculations indicate that $10^{10}$ interactions will produce 1 mJ/g of heating.

The effects of beam hitting the superconducting - magnet vacuum - chamber itself are reduced by certain simple measures. For instance, if the vacuum chamber wall is moved away from the superconducting coils, energy density is reduced because the shower can diffuse in the distance it must travel between the vacuum wall and the coil. Of the order of $10^{8}$ 1000-GeV particles must hit at one point in a bending magnet to deposit a peak of 1 mJ/g in energy. Figure 13-7 illustrates this reduction, as well as that gained by a plug in the magnet.

Further reduction of magnet sensitivity seems possible if collimator arrangements are located in the quadrupole assemblies as indicated in

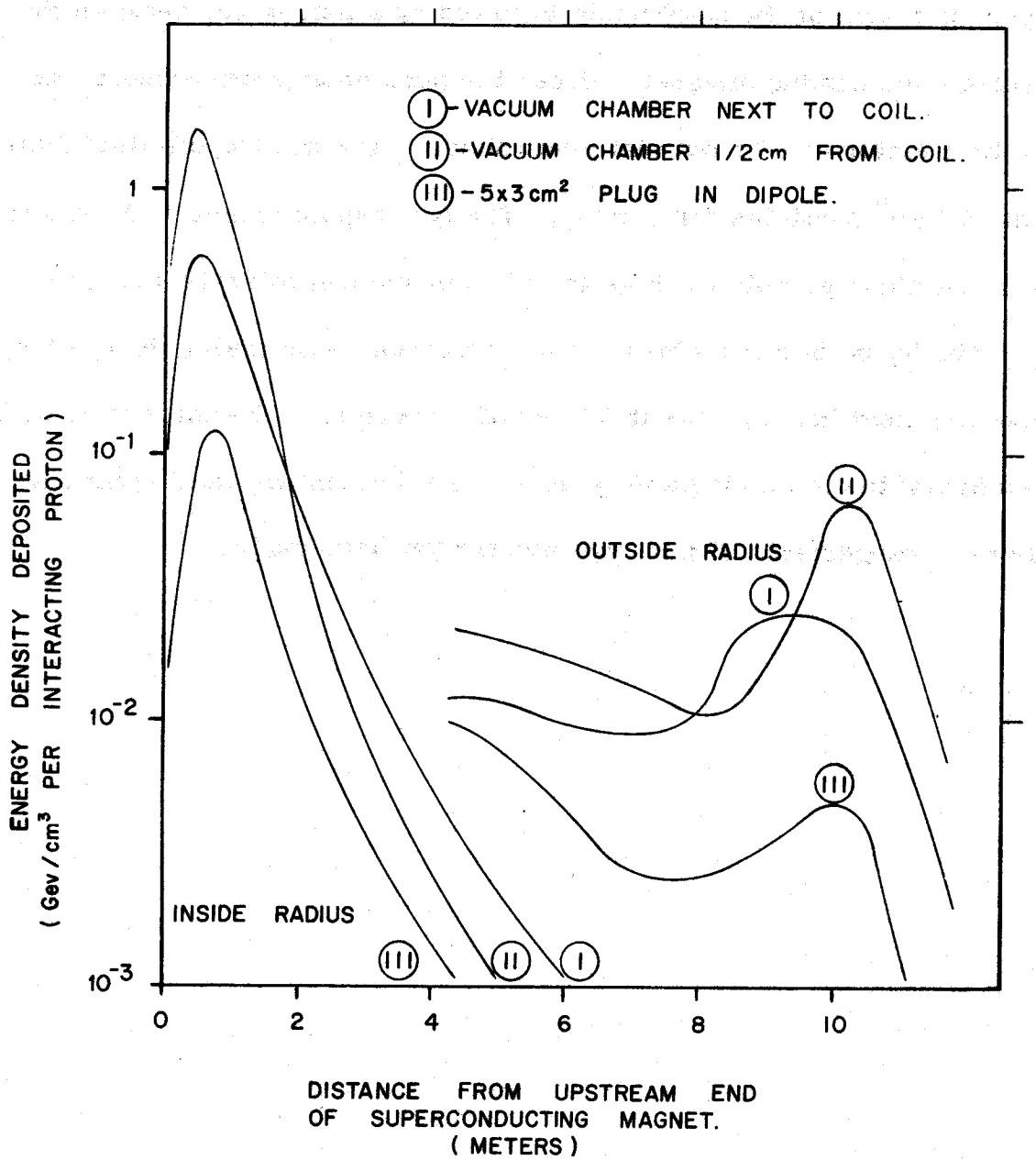


Fig. 13-7. Effects of different vacuum-chamber positions on energy deposition. The incident proton hits the upstream end of the dipole vacuum chamber or plug on the inside radius.

Fig. 13-8. Results for this case are shown in Fig. 13-9. A short primary scraper upstream of the quadrupole followed by a longer one between the quadrupole and bending magnet reduces the peak energy deposited in the dipole by a factor of 10 from that given above. The quadrupole itself can tolerate $5 \times 10^8$ particles for 1 mJ/g. The quadrupole magnets are not run as near the short sample limit as the dipoles and can tolerate a larger energy density before quenching. The correction coils inside the quadrupoles receive the most heating, but it is less of a problem if the correction coils quench than if the main magnets quench. The determination of optimum shielding arrangements of this type has not yet been made.

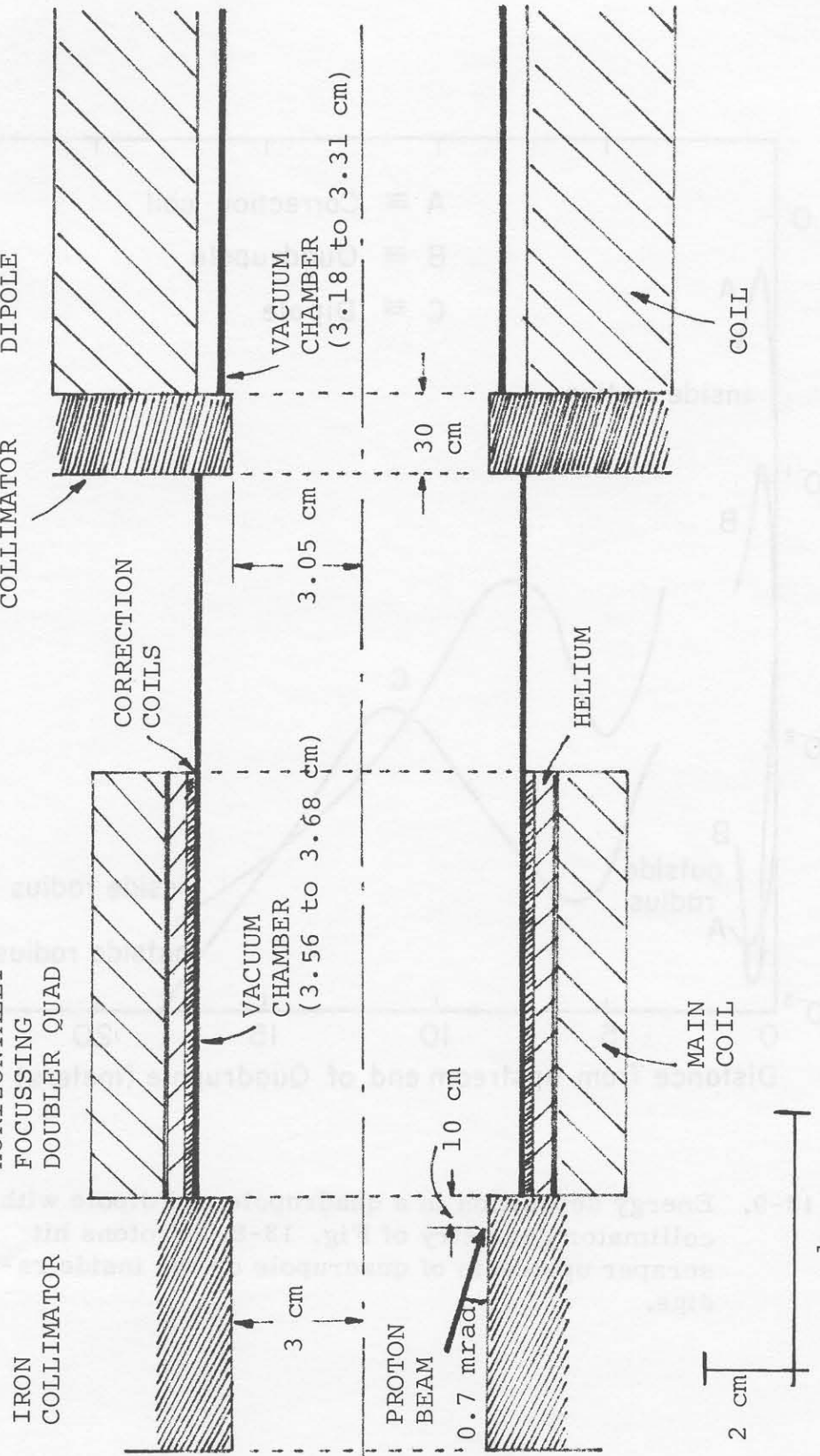


Fig. 13-8. Collimator geometry in quadrupole assembly used in calculations of Fig. 13-9.

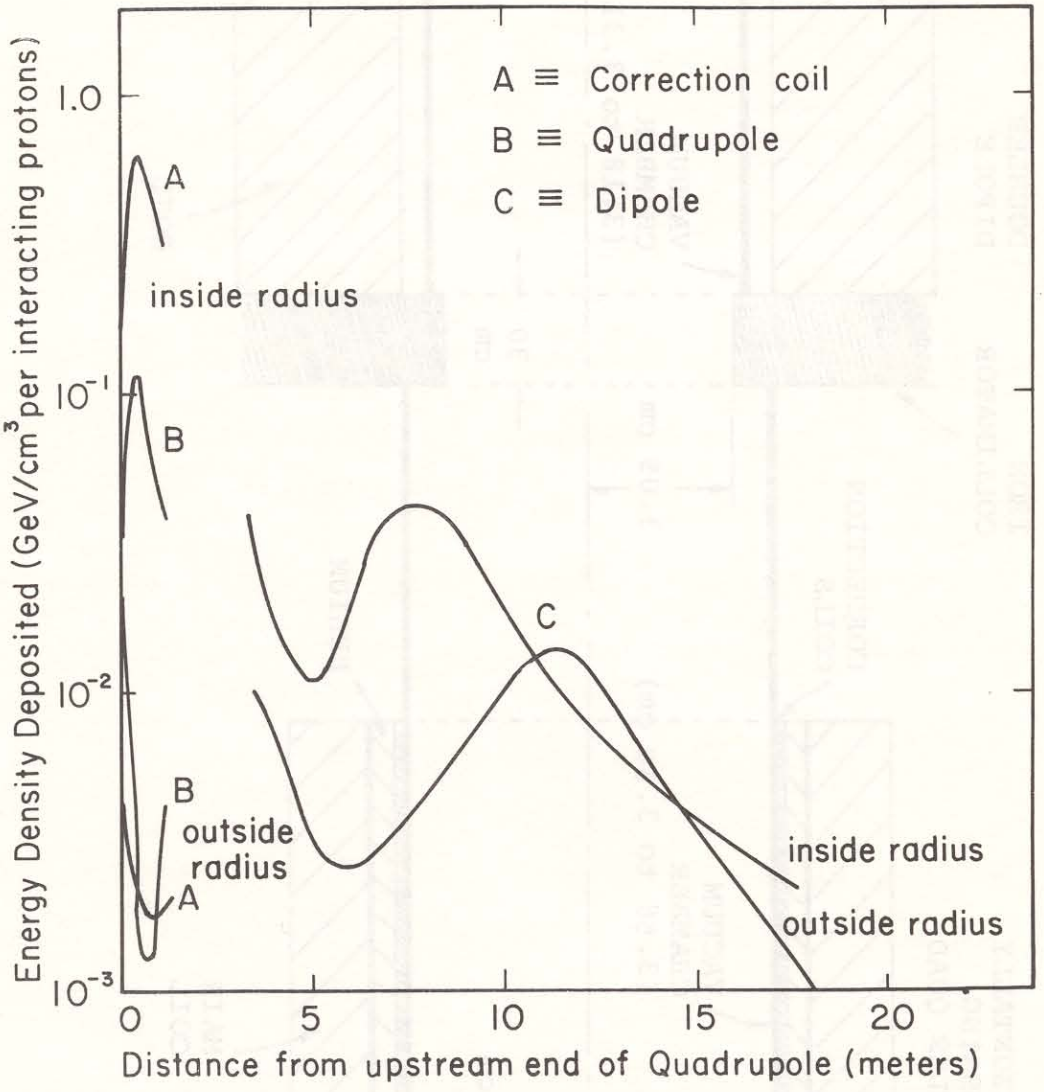


Fig. 13-9. Energy deposition in a quadrupole and dipole with collimator geometry of Fig. 13-8. Protons hit scraper upstream of quadrupole on the inside radius.

## References

[1] H. Edwards, paper submitted to the HEPAP Committee, Woods Hole Meeting, June 1977.

[2] B. Cox, P. O. Mazur, and A. Van Ginneken, Sensitivity of an Energy Doubler Dipole to Beam-Induced Quenches, Fermi National Accelerator Laboratory Internal Report TM-828-A, November 1978.

[3] H. Edwards, C. Rode, and J. McCarthy, IEEE Trans. Magn. 1, 666 (1977).

[4] A. Van Ginneken, CASIM - Program to Simulate Hadronic Cascades in Bulk Matter, Fermi National Accelerator Laboratory Report FN-272, January 1975.

[5] H. Edwards, S. Mori, and A. Van Ginneken, Studies on Radiation Shielding of Energy Doubler Magnets (1), Fermi National Accelerator Laboratory UPC No. 30, December 27, 1978.

H. Edwards, S. Mori, and A. Van Ginneken, Supplement to UPC 30, Fermi National Accelerator Laboratory UPC No. 40, January 12, 1979.

H. Edwards, S. Mori, and A. Van Ginneken, Supplement 2, of UPC No. 40, February 1979.